

## *Estimation of Body Structure by Biomechanical Impedance*

Hisao OKA                      Takashi FUKUDA

(Received January 27, 1995)

### **SYNOPSIS**

In the stiffness evaluation from the skin surface, the body structure under the skin, like a bone and muscle, influences on the measurement results. The authors developed the measurement system of biomechanical impedance with applying a vibration of acoustic frequency onto the body surface. We measured the viscoelasticity of the silicone-gel model, which involves metal blocks, from the gel surface by using this system. The internal structure of model is estimated from the relation between the viscoelasticity and the distance from the gel surface to the internal block. Applying this method, the shape of ribs of the right chest are estimated. The shapes and viscoelasticity of silicone-gel tumor model, which has two different tumors, are also estimated.

### **1. INTRODUCTION**

The clinical medicine in the present time is assisted by an engineering technique and the engineering technique is one of the pillars which support a medical service. A medical imaging system, which is one of these techniques, has not be realized without a support of an electronic engineering technique. To observe an internal constitution of the human body, there are some technique: using a nuclear magnetic resonance (MRI); imaging a distribution of X-ray absorption at each spot by making X-ray penetrate in the living body (X-ray CT); modulating ultrasonic pulse to brightness (ultrasonic diagnosing equipment) etc. Each of them has its merits and demerits<sup>(1)</sup>.

The clinical doctors examine a stiffness of the living body by manual palpation. Though it is highly sensitive, it is based on their experiences. Therefore it is important to express quantitatively and objectively a stiffness by measuring the physical properties of the living body. In the stiffness evaluation from the skin surface, an internal structure under the skin, like a bone or muscle, influences the measurement results, and a different results from the stiffness itself is almost obtained<sup>(2)</sup>. This suggests conversely an estimation of the internal body structure from the skin surface.

This paper deals with an estimation of a body structure and viscoelasticity under the skin surface, by using the acoustic vibration. We had measured the viscoelasticity of the silicone-gel models, which involve metal blocks, from the gel surface by using the above measuring system. The internal structure of the models is estimated from the relation between the viscoelasticity and a distance from the gel surface to internal block. This method is also applied to an estimation

of the shape of right chest ribs. Next the viscoelasticity of silicone-gel tumor model, which has two different tumors ( silicone-gel hemispheres ), is measured from the gel surface. Applying the relation between the viscoelasticity and the distance from the surface of silicone-gel model, which has two different stiffness strata, the shape and the viscoelasticity of internal hemispheres are estimated.

## 2. MEASUREMENT SYSTEM OF MECHANICAL IMPEDANCE

Fig.1 shows a block diagram of measurement system of mechanical impedance<sup>(3)</sup>. The silicone-gel model / skin surface is randomly vibrated at 30-1000 Hz by using an electrodynamic actuator of measuring probe, and the force  $f(t)$  and acceleration  $a(t)$  at the driving point are detected by using the impedance-head of the probe. The  $f(t)$  and  $a(t)$  is converted from an analog signal into a digital signal, and input to a personal computer. These are transformed to  $F(j\omega)$  and  $A(j\omega)$  by Fast Fourier transform, and the mechanical impedance of the model or skin is calculated as follows:

$$Z(j\omega) = \frac{F(j\omega)}{V(j\omega)} = \frac{F(j\omega)}{A(j\omega)/j\omega} = j\omega \frac{F(j\omega)}{A(j\omega)} \quad (1)$$

On the other hand, the radiation impedance of the vibrating sphere in the viscoelastic and incompressible medium, and in the case of low frequency, is proposed by Oestreicher<sup>(4)</sup>.

$$Z(j\omega) = 6\pi a^2 \sqrt{\frac{\rho(\sqrt{\mu_1^2 + \omega^2 \mu_2^2} + \mu_1)}{2}} + 6\pi a \mu_2 + j\omega \frac{2\pi a^3 \rho}{3} \\ + j6\pi a^2 \sqrt{\frac{\rho(\sqrt{\mu_1^2 + \omega^2 \mu_2^2} - \mu_1)}{2}} + \frac{6\pi a \mu_1}{j\omega} \quad (2)$$

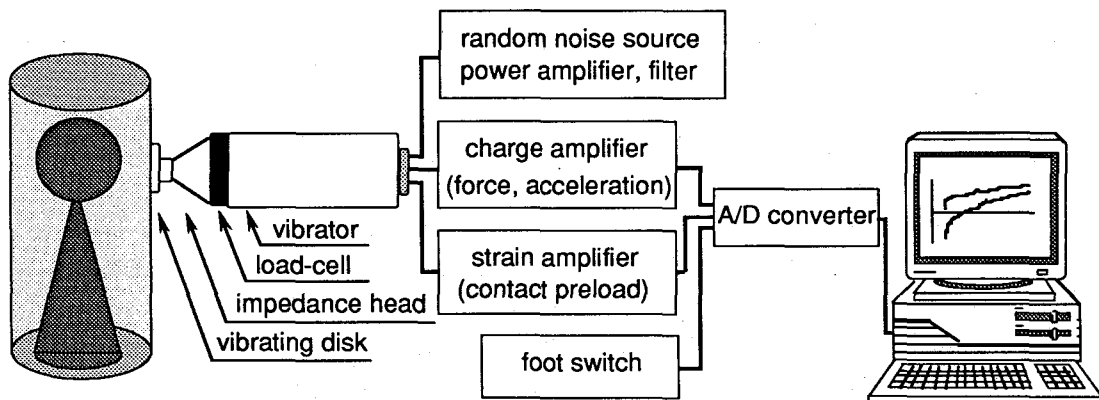


Fig. 1 Measurement system of mechanical impedance.

In this study, the radiation impedance, which is used in the viscoelasticity calculation, is theoretically half, because the model and skin are driven from the surface by the vibrating disk. The measured impedance spectrum is curve-fitted and then the shear elasticity  $\mu_1$ , shear viscosity  $\mu_2$ , effective vibrating radius  $a$  and medium density  $\rho$  (constant) are obtained<sup>(5)</sup>. Fig.2 shows that an impedance spectrum changes from the solid line to the dotted line, because it is influenced by the body structure near the measuring point and the apparent viscoelasticity is obtained by curve-fitting the dotted line.

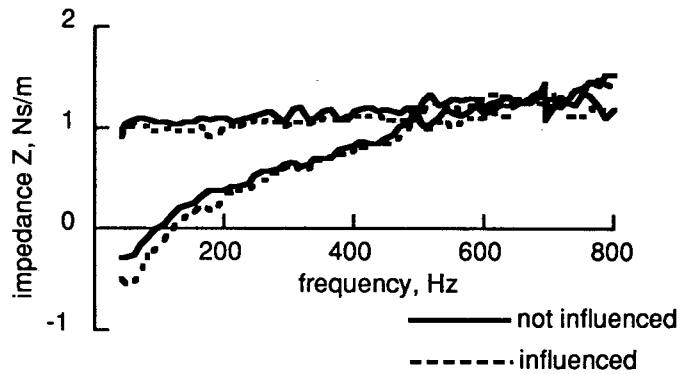


Fig.2 Mechanical impedance spectrum influenced internal structure.

**3. ESTIMATION OF INTERNAL STRUCTURE**

**3.1 Silicone-gel model**

Fig.3 shows two silicone-gel models, S(sphere)-C(cone) and S-C-C(cube) model. The tactility of used silicone-gel (KE1052, Shin-Etsu Co.) is not unlike human skin. The vibrating disk of probe is 10mm in diameter and the contact preload to gel surface is 10gf. The measured point of gel surface are 15×17 (S-C model) with a space of 10mm in the axial direction and 5mm in the circumferential direction and 39×34 (S-C-C model) with a latticed space of 5mm. The apparent  $\mu_1$ ,  $\mu_2$  and  $a$  is calculated by the curve-fitting of the obtained mechanical impedance spectrum.

**3.2 Estimation of distance**

Fig.4 shows the obtained viscoelasticity and  $d$  (theoretical distance from the surface) along the measuring line in the axial direction of silicone-gel model. It shows that the elasticity  $\mu_1$ , and effective vibrating radius  $a$  decreases, and the viscosity  $\mu_2$  increases, as the distance

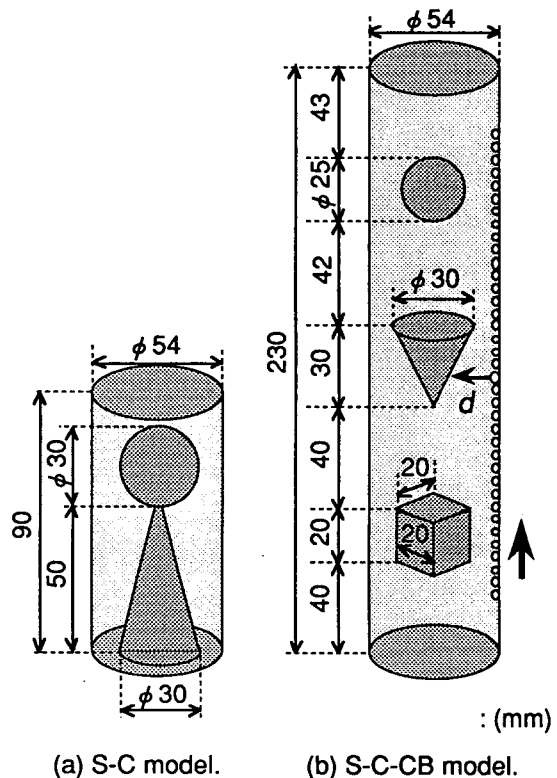


Fig.3 Silicone-gel model.

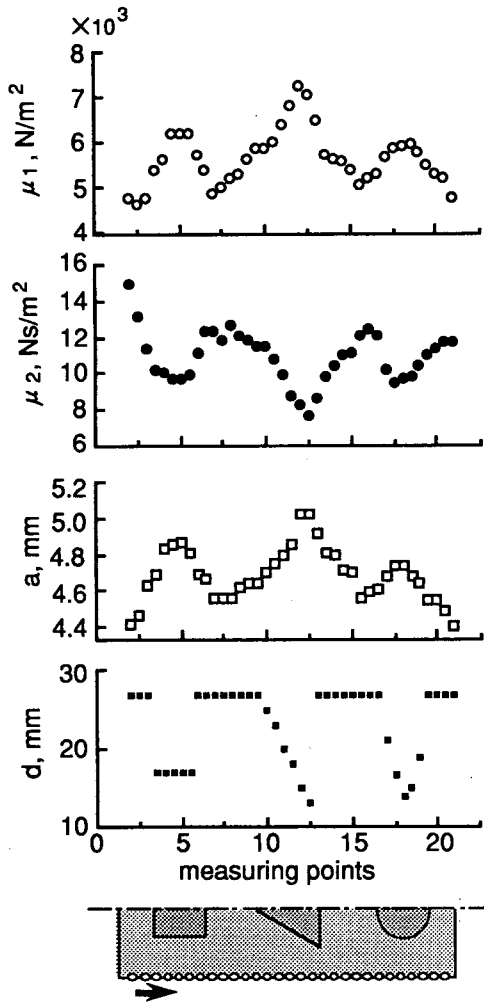


Fig.4  $\mu_1$ ,  $\mu_2$ ,  $a$  obtained from the impedance of S-C-CB model and theoretical distance.

to the internal structure increases. The obtained viscoelasticity is related to the distance to internal structure. By using the effective vibrating radius  $a$ , the distance from surface to internal structure is possible to be estimated. Fig.5 shows a relation between the distance  $d$  from the gel surface and the effective vibrating radius  $a$ , which signifies the dependence of viscoelasticity on internal structure. Then the  $a$  obtained from the result should give an estimated distance from the gel surface. Fig.6 shows a 3-D reconstructed image of internal structure of S-C model (a) and S-C-C model (b). Each sectional circle which shows the estimated distance is smoothed by a moving average method.

### 3.3 Application to the living body

When applying this method to the living body, the relation between the effective vibrating

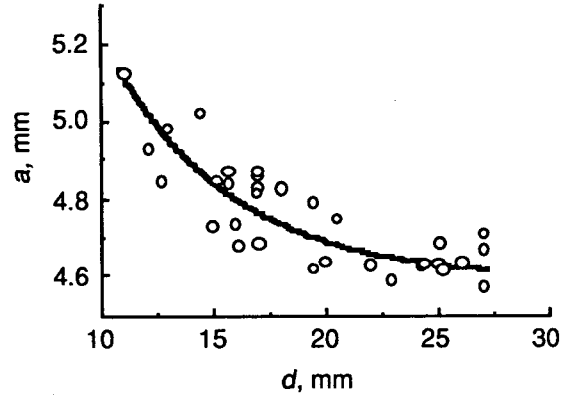


Fig.5 Effective vibrating radius and the distance from gel surface.

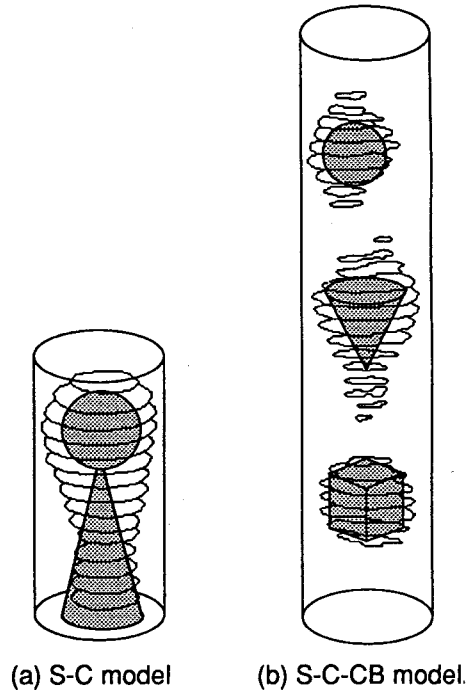


Fig.6 3-D reconstructed image of S-C and S-C-CB model.

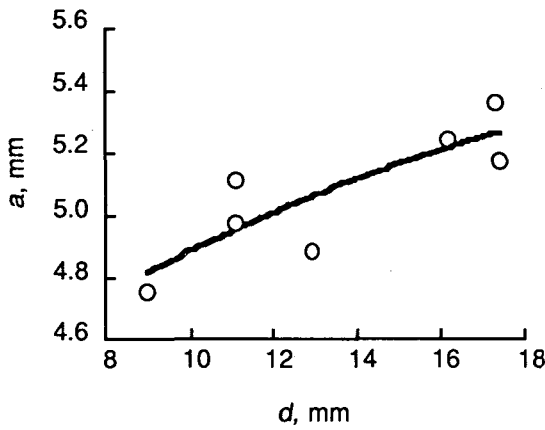


Fig.7 Effective vibrating radius and the distance from skin surface of chest.

radius  $a$  and theoretical distance on the living body (where a distance to the bone) should be obtained beforehand. The distance  $d$  between the ribs and the skin surface near the measured region has been observed by using an ultrasonic diagnosing equipment. The relation between this distance  $d$  and the effective vibrating radius  $a$ , which is obtained at same point, is shown in Fig.7. The biomechanical impedances at  $11 \times 7$  points on the ribs of right chest in Fig.8 with a latticed space of 10mm are measured and  $\mu_1$ ,  $\mu_2$  and  $a$  are obtained. The vibrating disk is 10mm in diameter and the preload is 10gf. The obtained  $a$  gives an estimated distance from the chest surface, by using the above relation between  $a$  and theoretical distance  $d$ . Fig.9 shows a 3-D reconstructed image of the ribs. The figure shows that the higher becomes a peak, the smaller becomes the estimated distance from surface. Fig.10 shows the 3-D imaging of the distance from skin surface, which has been observed by the ultrasonic equipment in the same measured point.

**4. VISCOELASTICITY ESTIMATION OF THE SILICONE-GEL MODEL**

Next a viscoelasticity estimation of inside material is dealt in the case that the internal material is pretty softer than the metal or bone.

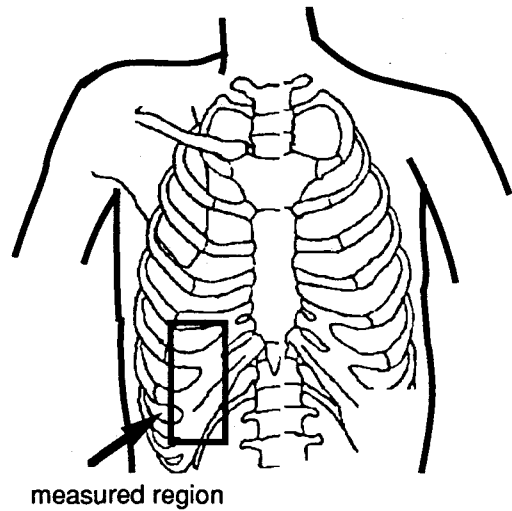


Fig.8 Measured region of right chest.

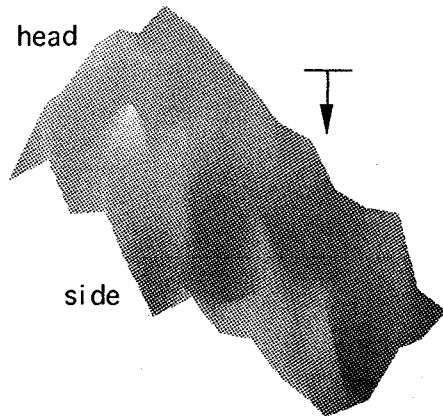


Fig.9 3-D reconstructed image of the ribs.

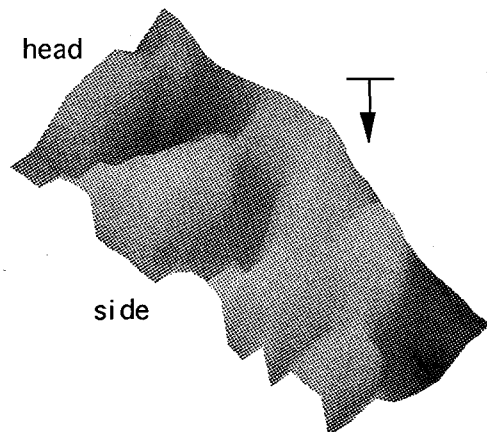


Fig.10 3-D reconstructed image by using ultrasonic diagnosing equipment.

**4.1 AB and AC silicone-gel model**

Fig.11 shows a silicone-gel model which has two different stiffness strata. Fig.11(a) shows a silicone-gel A, B and C is put in the container which has a slope inside in it. The silicone-gel B is harder than the silicone-gel

A and the silicone-gel C is softer than the silicone-gel A, the penetration of gel A is 70, the gel B is 50, the gel C is 90. Fig.11(b) shows a silicone-gel AB and AC model that the gel A is put in the container, which has a slope similar to the above models, by using the gel B and C. The mechanical impedance of these models is measured with a space of 5mm in the direction that the distance to the lower structure increases. The vibrating disk is 10mm in diameter and the contact preload onto the gel surface is 10gf. Fig.12 shows the relation between the vertical distance to the lower structure and the apparent elasticity  $\mu_1$ , the viscosity  $\mu_2$  and the effective vibrating radius  $a$ , which are obtained by measuring A, B, C, AB and AC silicone-gel model. It shows that a influence of the lower gel does not appear when the distance to the lower gel is longer than 30mm. Then it is possible to estimate the viscoelasticity of lower gel by using this relation, if the distance to the lower gel is shorter than 30mm.

**4.2 Viscoelasticity estimation of AB and AC model**

The viscoelasticities of silicone-gel AB and AC model should be regarded to be coupled in series each other, as shown in Fig.13. First the elasticity of AB model is treated as a real elasticity (a convergent value) of the A and B model itself,  $\mu_{1A_n}$  and  $\mu_{1B_n}$ . A weight of  $\mu_{1A_n}$  and  $\mu_{1B_n}$ , is fixed for  $\alpha$  1,  $\beta$  1. Similarly, a real viscosity (a convergent value) is treated as  $\mu_{2A_n}$  and  $\mu_{2B_n}$  and the viscoelasticity  $\mu_1$  and  $\mu_2$  of AB model is obtained as follows :

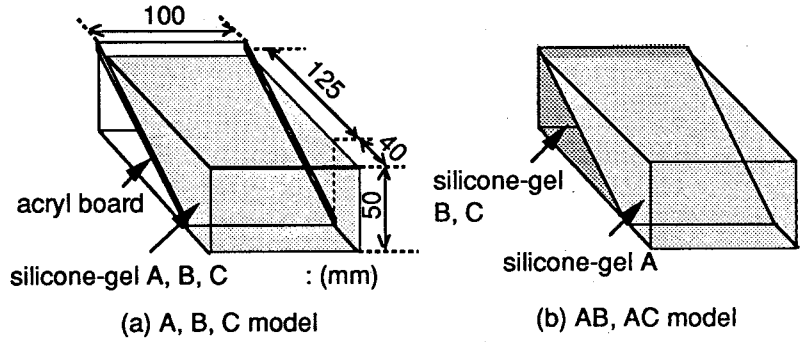


Fig.11 A, B, C, AB and AC silicone-gel models.

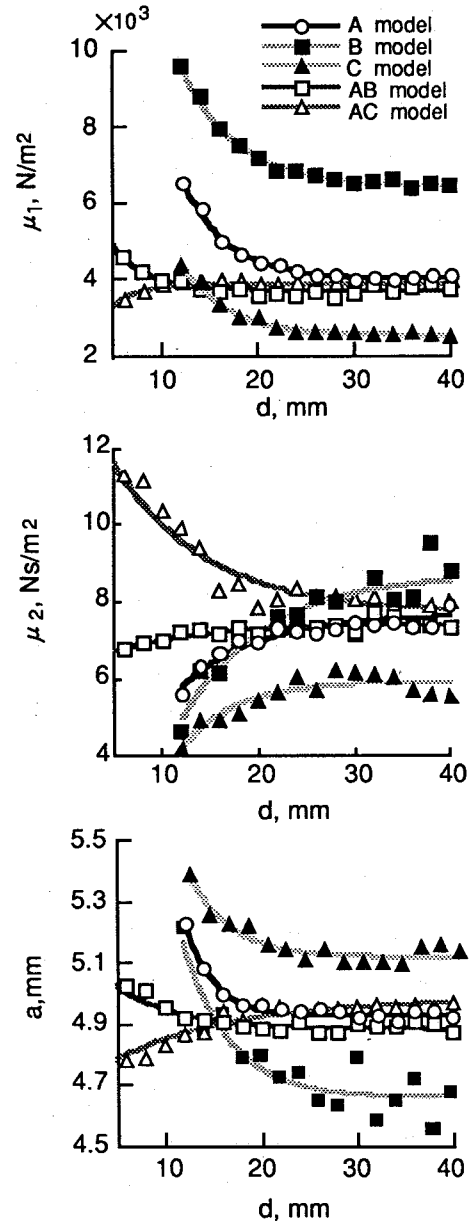


Fig.12 Distance and an apparent  $\mu_1$ ,  $\mu_2$ , and  $a$ .

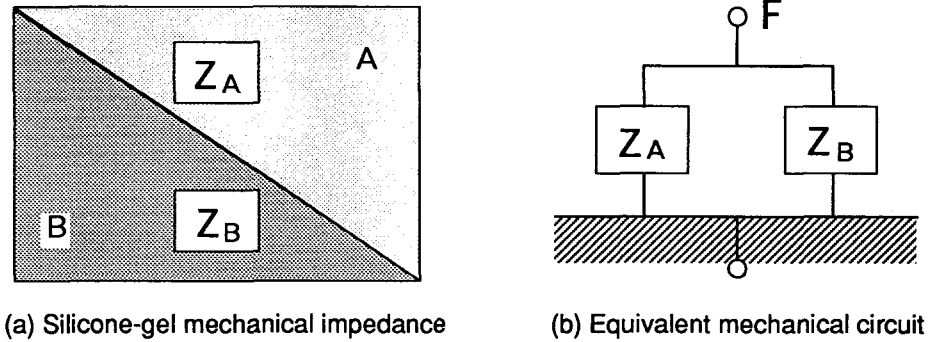


Fig.13 Mechanical structure of AB model.

$$\frac{\alpha_1}{\mu_{1An}} + \frac{\beta_1}{\mu_{1Bn}} = \frac{1}{\mu_1} \tag{3}$$

$$\frac{\alpha_2}{\mu_{2An}} + \frac{\beta_2}{\mu_{2Bn}} = \frac{1}{\mu_2} \tag{4}$$

In the decision of  $\alpha$  and  $\beta$ , the second term of the left side of Eqn.3 is ignored, the measurement result of A model is substituted for  $\mu_1$  and then the weight of elasticity  $\alpha_1$  is decided. The weight  $\beta_1$  is decided by substituting the  $\alpha_1$  and the measurement result of AB model. Similarly  $\alpha_2$  and  $\beta_2$  are decided. Fig.14 shows  $\alpha$  and  $\beta$ , which is related to the distance to the lower material. When the silicone-gel model is made of the same medium, the viscoelasticity of internal gel itself can be estimated by using Eqn.3 and 4.

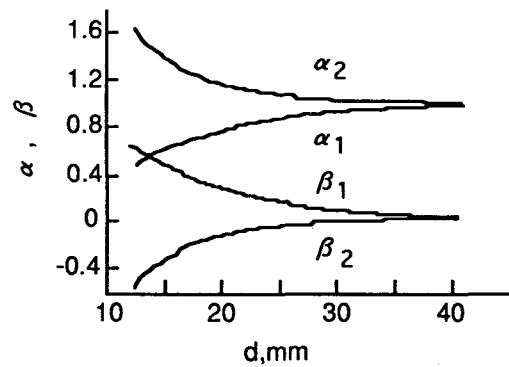


Fig.14 Distance and  $\alpha, \beta$ .

### 5. APPLICATION TO THE SILICONE-GEL TUMOR MODEL

Fig.15 shows a silicone-gel tumor model, which has two different tumor (hemisphere which is made of gel B and C), by using the silicone-gel A, B and C used in the above chapter. The mechanical impedance is measured at  $19 \times 40$  point on the tumor with a latticed space of 5mm. The vibrating disk is 10mm in diameter and the preload is 10gf.

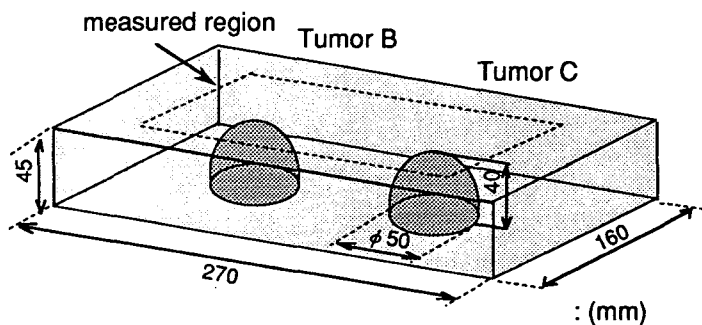


Fig.15 Silicone-gel tumor model.

**5.1 Structure estimation of the tumor**

The effective vibrating radius  $a$ , obtained from the measurement of the tumor model, should give the estimated distance to the tumor. By using the relation between the distance and the effective vibrating radius of AB and AC model, Fig.16 shows a 3-D reconstructed image of internal structure of the tumor model. The figure also shows a cross section between 1-1'. The shape of the tumors could be estimate till only 20mm of depth, but the resolution should be improved by changing an amplitude of vibration, the preload, the diameter of vibrating disk and a measuring space.

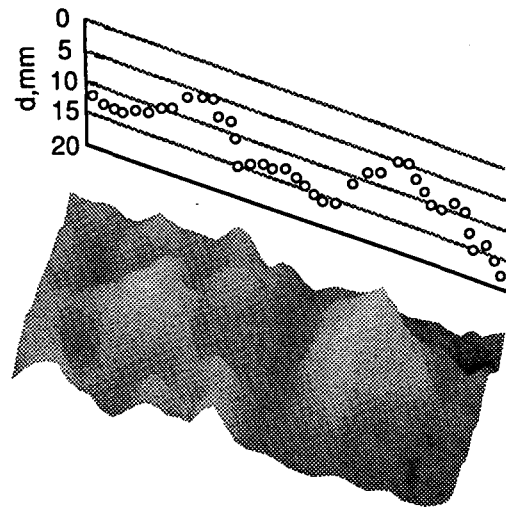


Fig.16 Reconstructed image of tumor model.

**5.2 Viscoelasticity estimation of tumor**

The  $\alpha_1$  and  $\beta_1$  is obtained from the estimated distance at the measuring point, They are calculated from the result of measurement  $\mu_1$  and the  $\mu_{1An}$ , which are known beforehand substitute for Eqn. 3. Then the elasticity  $\mu_{1Bn}$  of tumor B is calculated. Similarly the viscosity  $\mu_{2Bn}$  of tumor B is calculated from Eqn. 4, and the viscoelasticity  $\mu_{1Cn}$  and  $\mu_{2Cn}$  of tumor C is also calculated. Fig.17 shows a internal viscoelasticity mapping of  $\mu_{1Bn}$ ,  $\mu_{2Bn}$ ,  $\mu_{1Cn}$  and  $\mu_{2Cn}$ , which are estimated at each measuring point. It shows that the estimated values vary a little, but the estimated value is larger around the tumor B, which is harder, and smaller around the tumor C,

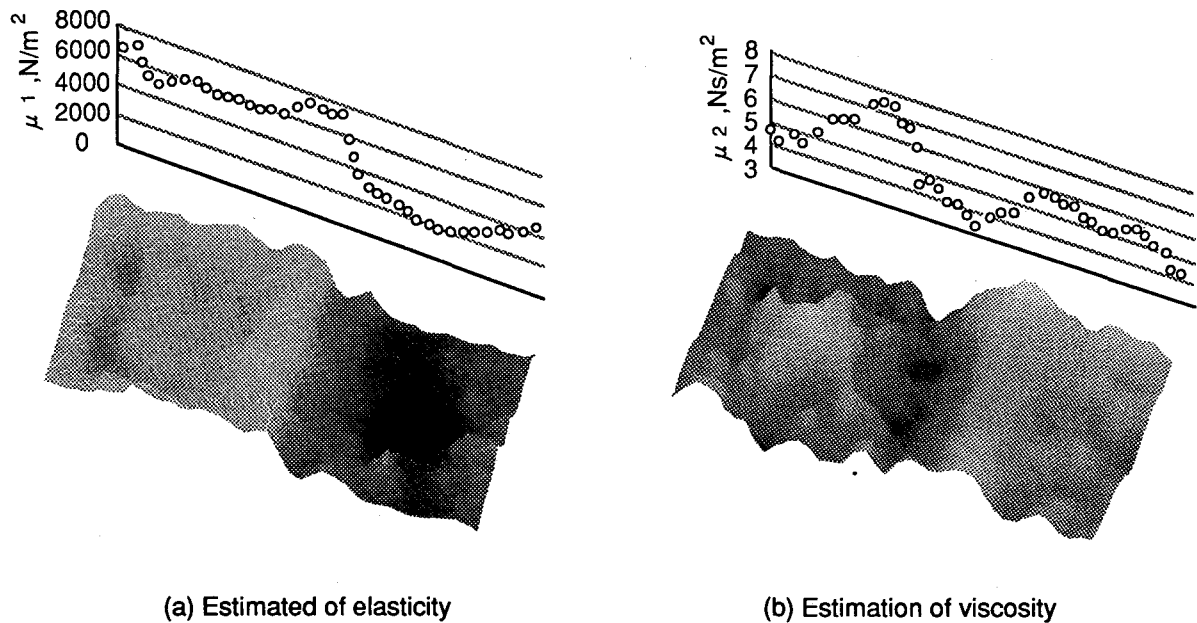


Fig.17 Viscoelasticity estimation of Tumor model.



which is softer. Table 1 shows the estimated  $\mu_1$  and  $\mu_2$  of tumor B and C, the real  $\mu_1$  and  $\mu_2$  of gel B and C and standard deviations of them. Each estimated value is smaller than the real viscoelasticity of the silicone-gel.

Table 1 Estimation of viscoelasticity of the A, B and C silicone-gel.

	gel A		gel B		gel C	
	real value	estimated value	real value	estimated value	real value	estimated value
$\mu_1$ (N/m <sup>2</sup> )	3940	4235 ( $\pm 34.5\%$ )	6432	6227 ( $\pm 6.5\%$ )	2542	2124 ( $\pm 9.6\%$ )
$\mu_2$ (Ns/m <sup>2</sup> )	7.7	4.77 ( $\pm 32.5\%$ )	8.68	7.13 ( $\pm 10.7\%$ )	5.89	5.24 ( $\pm 3.4\%$ )

## 6. CONCLUSIONS

The viscoelasticity is measured from the surface of silicone-gel model by the measurement system of mechanical impedance. The elasticity  $\mu_1$ , and effective vibrating radius  $a$  decreases, and the viscosity  $\mu_2$  increases, as the distance to the internal structure increases. On basis of the distance from the surface and the effective vibrating radius  $a$ , it is possible to obtain the 3-D reconstructed image of internal structure of the silicone-gel model and the ribs of right chest. By using the relation between the distance and the viscoelasticity of silicone-gel AB and AC model, the shape and the viscoelasticity of internal tumor of silicone-gel tumor model are also estimated.

## ACKNOWLEDGMENT

The authors would like to acknowledge the Scientific Research Fund of the Japanese Ministry of Education (No. 06650470) for supporting research for this paper.

## REFERENCE

- (1) Geddes, L. A. and Baker, L. E. : Wiley-Interscience, New York, (1989)
- (2) Oka, H. and Yamamoto, T. : Med. & Biol. Eng. & Comput., 25 (1987) , 631, 637.
- (3) Oka, H., Yamamoto, T. and Okumura, Y. : Innov. Tech. Biol. Med., 8 (1987) , 1, 11.
- (4) Oestreicher, H. L. : J. Acoust. Soc. Am., 23 (1951) , 707, 712.
- (5) von Gierke, H. E., Oestreicher, H. L., Franke, E. K., Parrack, H. O. and von Witten, W. W., 4, (1952) , 886, 900.